Connectivity-aware sectional visualization of DTI volumes

Çağatay Demiralp
Brown University

Daniel Acevedo
Brown University

Song Zhang
Mississippi State University.

David F. Tate
Harvard University

Stephen Correia
Brown University

David H. Laidlaw
Brown University

August 7, 2007

Abstract

We present three methods for visualizing cross-sections of diffusion tensor magnetic resonance imaging (DTI) volumes. The goal of our methods is to effectively bring 3D out-of-plane connectivity information into the cross-section plane, as inspecting 2D cross-sections is a common practice for scientific data exploration. In order to derive the connectivity information associated with a cross-section, we first sample points (seeds) on a regular grid on the cross-section and then, from each point, generate integral curves following the principal eigenvector of the underlying diffusion tensor field in both directions. We quantify how these curves relate to each other by computing an anatomically motivated pairwise distance measure between them and assemble the measures into a distance matrix. All of the three methods visualize these 3D distance relations on the cross-section plane. Our first method (*Bohemian coloring*) uses color changes proportional to the distances in the L*a*b* color space; our second method (*icon layering*) uses both color changes and icons of varying size and layout; our third visualization uses line segments rendered with different thicknesses and shades (*edge rendering*). All of our methods provide a way to visually segment 2D slices of DTI data with respect to the integral curves crossing the slice plane. We demonstrate our methods in visualizing the mid-sagittal cross-section of the corpus callosum in the brain. Experts report that our methods may facilitate demarcation of subtler anatomical-functional divisions of the corpus callosum and can be useful in quick diagnosis of subtle but critical changes in the number and shape of the neuro-fibers due to injuries. Also, a particular contribution of the current work is to introduce a continuous 2D color mapping technique based on a new geometric model, flat-torus, providing approximate perceptual uniformity and can be repeated an arbitrary number of times in both directions to increase sensitivity.

1 Introduction

Diffusion-Tensor Magnetic Resonance Imaging (DTI) enables the exploration of fibrous tissues such as brain white matter and muscles non-invasively *in-vivo*. It

exploits the fact that water in these tissues diffuses at faster rates along fibers than orthogonal to them. However, the multivalued nature of DTI data poses challenges in visualizing and understanding the underlying structures. Integral curves that represent neural pathways by showing paths of fastest diffusion are among the most common information derived from DTI volumes. They are generated by tracking the principal eigenvector of the underlying diffusion tensor field in both directions. They are often visualized with streamlines or variations of streamlines (streamtubes and hyperstreamlines) in 3D.

In this paper, we present three new methods for visualizing cross sections of DTI volumes that incorporate the 3D out-of-plane connectivity information typically conveyed by the integral curves. Slice-based 2D visualizations of scientific data are generally effective, fast and synoptic [1, 6]. Also, looking at 2D cross-sections is still the most common practice by far among scientists and physicians for data exploration. Furthermore, there is some anecdotal evidence that incorporation of 2D cross-sections in 3D visualizations of medical data sets data is preferred by the same group [2]. For each of our three visualization methods we show exam-

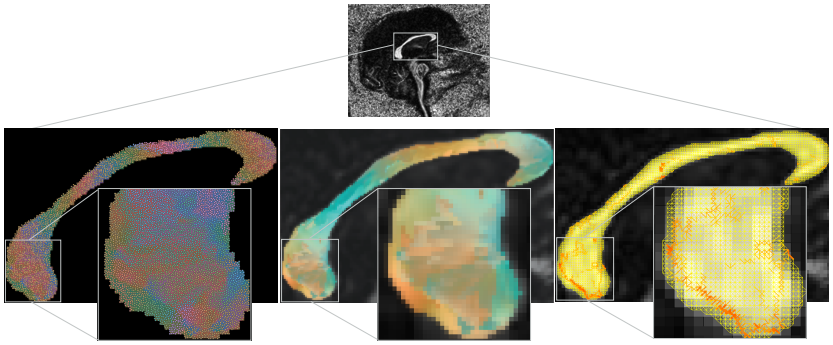

Figure 1: *Icon layering* (left), *Bohemian coloring* (middle), and *edge rendering* (right) visualizations of the mid-saggital plane of the corpus callosum in a normal volunteer's brain.

ple visualizations of the corpus callosum in the mid-sagittal plane of three normal volunteers. The corpus callosum is the largest white matter structure connecting the left and right hemispheres in the brain. It is a target for clinical and neuroscience research into normal developmental vs. pathological changes in white matter integrity across the lifespan and the functional correlates of those changes. The fibers in the corpus callosum usually project to homologous regions in opposite hemispheres on an anterior-posterior gradient, but heterologous connections also exist. Accordingly, distinct cross-sectional regions of the corpus callosum may contain fibers that subserve specific cognitive or behavioral functions mediated by the cortical regions to which they project. Proxy measures (e.g., thickness, volume, area, shape) of the health of these cross-sectional regions may correlate with measures of the cognitive and behavioral functions they subserve. In fact, the corpus callosum has been shown to differ on such measures by handedness, gender, and age as well as in diseases such as Alzheimer's disease and schizophrenia. Until fairly recently, structural clinical neuroimaging studies on the corpus callosum either in development, aging, or disease have been based on quantitative

measurements obtained from conventional anatomic MRI or computed tomography (CT) images. However, because there are no visually distinct structural or functional segments of the corpus callosum, most of these studies have relied on rather arbitrary divisions. The advent of DTI fiber tracking provides an opportunity to demarcate and measure callosal subdivisions that are based on spatial trajectory of the fibers, an approach that should permit greater specificity in determining anatomic-functional correlations within the corpus callosum.

We presented preliminary results involving two of our methods as a short paper in [3]. In this paper we give a more complete coverage our work with an addition of a new layered icon-based visualization method.

The ideas and techniques used in our work relate to previous works from different areas in multiple fields. In the following section we discuss these related works. Then, we give details on the three visualization methods in section 2.1 and present the results of their applications with an evaluation by experts in section 3. We finish the paper by summarizing our work and contributions, and by concluding in section 4.

2 Methods

The goal of our visualization methods is to effectively combine 3D out-of-plane connectivity information into the cross-section plane. We start with measuring how a region of interest (ROI) in given cross-section relates (connects) to the other parts of the data.

2.1 Measuring Connectivity

In order to derive the connectivity information associated with a cross-section, we first sample points (seeds) on a regular grid on the cross-section and then, from each point, generate integral curves following the principal eigenvector of the underlying diffusion tensor field in both directions (see Figure 2). Integral curves generated from DTI volumes are solutions to the first-order differential equation

$$\frac{dC}{ds} = \vec{v}_1(C(s)) \tag{1}$$

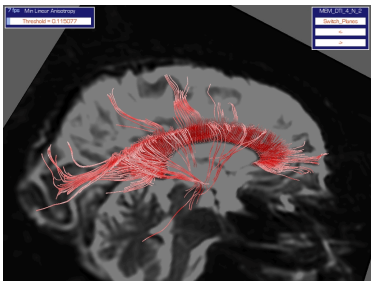

Figure 2: 3D view of the mid-saggital plane of the corpus callosum with the integral curves (represented with streamtubes) generated by sampling seed points on a regular grid in the slice plane.

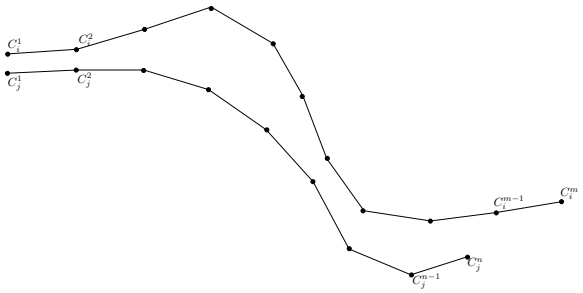

Figure 3: Polyline representations of two integral curves C_i and C_j

,where s parameterizes the curve and v_1 is the principal eigenvector at the point $C(s) = (x(s), y(s), z(s))$. We compute the integral curve $C(s)$ passing through a given seed point $C(0)$ (initial conditions) by integrating the above equation for $s > 0$ and $s < 0$ (i.e., both directions from the seed point).

2.2 Distances Between Integral Curves

We quantify how integral curves relate to each other by computing an anatomically motivated pairwise distance measure between them and assemble the measures into a distance (similarity) matrix.

There have been different distance measures proposed for integral curves generated from DTI volumes [5]. In the current work we adapt a measure proposed by Zhang *et al.* with a slight modification [8]. The measure is anatomically motivated in that it is designed to increase whenever one path has points that are not near the other path. As these curves are approximations for neural pathways, our measure tries to capture how much any given two curves follow a similar (or dissimilar) path. Note that our measure does not necessarily satisfy the triangle inequality, therefore, it is not a metric. Given any two integral curves C_i and C_j that are represented as polylines with m and n vertices respectively (like the ones shown in Figure 3), we first find mean distances d_{ij} and d_{ji} then, determine the maximum of these two distances as the distance D_{ij} between the two curves:

$$d_{ij} = \frac{\sum_{k=1}^{m} \text{dist}(C_i^k, C_j)}{m} \tag{2}$$

$$d_{ji} = \frac{\sum_{k=1}^{n} \text{dist}(C_j^k, C_i)}{n} \tag{3}$$

$$D_{ij} = D_{ji} = \max(d_{ij}, d_{ji}) \tag{4}$$

The function $\text{dist}(p, C)$ returns the shortest Euclidean distance between the point p and curve C. We compute distance between each pair of integral curves as we denoted and assemble the measures to create a distance matrix. The distance matrix is a real positive symmetric matrix with zeros along the diagonal.

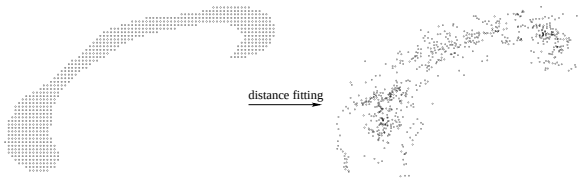

Figure 4: Seed points are adjusted so that Euclidean distances between the points on the plane reflect the distances between their associated integral curves.

2.3 Embedding Curves into 2D Plane

Our *icon layering* and *Bohemian coloring* methods aim to reflect the boundaries in distance changes between integral curves as perceptual boundaries. For this, we first embed the distance relations represented by the distance matrix into a plane where each 2D point uniquely represents an integral curve, and Euclidean distances between the points are approximations to the distances between the corresponding integral curves. The seed points are a natural initialization for our embedding algorithm. We lay out the seed points on a plane (embedding plane) and adjust their positions using a simple mass-spring-based optimization algorithm so that the calculated distances between their associated integral curves are best preserved locally. Figure 4 illustrates how seed point coordinates change after running the optimization algorithm. We coordinate-transform the adjusted points using

2.4 Flat-torus:A New Model for Bivariate Colormapping

We propose flat-torus as a new geometric model for bivariate color mapping. We "wrap" the embedding plane onto a flat-torus. A flat-torus in 4-space is a Cartesian product of two circles in R^2. It can be obtained by a mapping $W : R^2 \rightarrow R^4$ such that

$$W(x,y) = (u,v,s,t) = (r_1 \cos x, r_1 \sin x, r_2 \cos y, r_2 \sin y) \tag{5}$$

where $r1$ and $r2$ are the radii of the circles. The flat-torus has 0 Gaussian curvature everywhere (i.e., is a developable surface), therefore a plane can be wrapped around it without distortion [4]. This is particularly useful because wrapping the embedding plane onto the flat-torus does not distort the embedded distances. One of the primary advantages of using flat-torus is that we can adjust the sensitivity of the color mapping by rescaling the data values (i.e., points on the plane) uniformly and wrapping around the two circles, determined by r_1 and r_2,continuously (see Figure 5).

2.5 Icon Layering

Our first visualization method *icon layering* wraps the planar representation generated by the embedding algorithm onto a flat-torus creating 4D (u,v,s,t) coordinates for the plane points and, then, superimposes one layer of circular icons over a colormapped plane using the 4D flat-torus representation. While we create the first layer by mapping u and v values to an equiluminant plane of the L*a*b* color space, we create the second layer by placing icons in a Poisson disk distribution

on the plane and coloring them by mapping s and t values to another plane of the L*a*b* color space. The mapping is simple:

$$(L_1*, a_1, b_1) = (c_1, a_0+u, b_0+v) \quad (6)$$
$$(L_2*, a_2, b_2) = (c_2, a_0+s, b_0+t) \quad (7)$$

This effectively means that we obtain the color for the first layer of our visualization by mapping the planar representation to (x,y) to a circle centered at (a_0,b_0) on $L=c_1$ plane and the color for the second layer of our visualization by mapping the same (x,y) to another circle centered again at (a_0,b_0) but on a different, $L=c_2$, luminance plane. Details on our icon-placement algorithm based on Poisson-disk distribution can be found in [7].

For the *icon layering* visualization examples shown in this paper (Figures 1,8, and 9), we use $L_1=c_1=64$ and $L_2=c_2=74$ luminance planes of the L*a*b* color space with $a_0=-10, b_0=20$ (see Figure 6) and a flat-torus with $r_1=r_2=40$.

2.6 Bohemian Coloring

Our second visualization method,*Bohemian coloring*, also wraps the planar representation generated by the embedding algorithm onto a flat-torus creating 4D (u,v,s,t) coordinates for the plane points. However, *Bohemian coloring* projects the flat-torus onto a a quartic surface called Bohemian Dome (see Figure 7) centered at (L_o, a_o+r_1, b_o) in a visible portion of the L*a*b* color space as follows:

$$(L*, a*, b*) = (L_o+t, a_o+r_1+u+s, b_o+v) \quad (8)$$

The colors for the paths are used to color the corresponding grid points on the original cross-section. The resulting image shows larger changes in color where neighboring integral curves differ more.

Note that this projection is not isometric. It has two lines of self-intersection (where different (x,y) points map to the same colors) as well as distorting the angles between the coordinate directions. We discuss this further in section 3. For the examples shown in this paper, we locate the projected Bohemian Dome in the

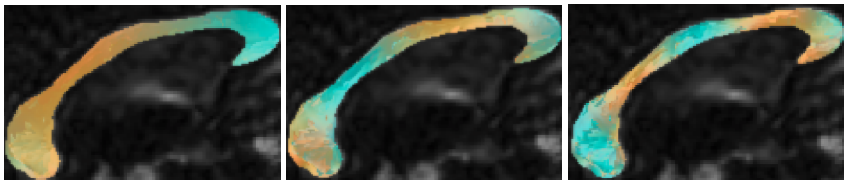

(a) low (b) medium (c) high

Figure 5: Flat-torus model allows adjusting the sensitivity of colormapping by rescaling the planar representation (embedding) of the integral curves and "wrapping" around the flat-torus as many times as needed. Pictures shows the visualization of the mid-sagittal plane of the corpus callosum using *Bohemian coloring* with increasing sensitivity.

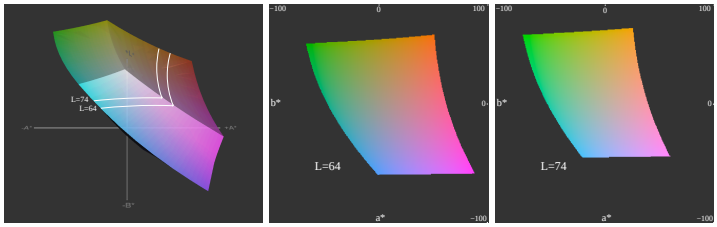

Figure 6: sRGB gamut in the L*a*b* space (left) and L*=65 (middle) and L*=75 (right) slices

L*a*b* interval $I = (I_L, I_b, I_c)$, where $I_L = [60, 80], I_a = [-50, 30], I_b = [-20, 60]$, and use $r_1 = 30$, $r_2 = 10$. Note that $L_0 = 70, a_0 = -10$, and $b_0 = 40$ follows.

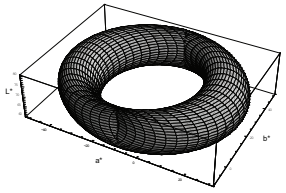

Figure 7: Bohemian Dome.

2.7 Edge Rendering

Our third visualization method lays out the grid points on the cross section and connects the neighboring points with edges that are rendered according to the distances between curves generated from these points. Note that we sample seed points on a rectilinear grid where the vertical and horizontal distances between the grid points are equal to δ. We define the seed points X_i and X_j to be neighbors if $||X_i - X_j||_2 = \delta$ or $||X_i - X_j||_2 = \delta\sqrt{2}$ (i.e., a seed point can have maximum 8 neighbors). Edges are drawn redder in color and thicker where neighboring seed points' integral curves differ more.

3 Results and Discussion

Figure 1 show the visualizations of the same normal person's corpus callosum with close-up views of the same region. Observe the correspondance between regions in *icon layering* and *Bohemian coloring*, and edges in *edge rendering*. Other results from two DTI brain data sets are shown in Figures 8 and 9.

It is important to note that the perceptual uniformity in *Bohemian coloring* is an approximation, because the flat-torus cannot be mapped to three dimensions isometrically. Our projection can deemphasize changes in certain regions of the flat torus. There are other projections that may be closer to isometric and it also may be possible to add a fourth perceptual dimension like texture to the three color dimensions, removing the need for a projection and preserving the properties of the flat

torus. Similarly, by mapping u,v and s,t coordinates to the two luminance planes of the L*a*b* color space, *icon layering* visualization overestimates distances.

3.1 Expert Evaluation

Current methods for visualizing corpus callosum from DTI data consist mainly of cross sectional views of scalar parameter maps such as fractional anisotropy (FA) or mean diffusivity (MD) or by fiber tractography. Each of these methods has strengths and weaknesses. For example, sagittal mid-section views of the corpus callosum in scalar maps provide a clear picture of its shape and boundaries. The entire corpus callosum or subregions can be sampled to obtain scalar values that provide insight into the structural integrity of the white matter fibers that comprise it. Unfortunately, these scalar maps are visually homogeneous and therefore provide no visual information about the trajectory of fibers in the corpus callosum or of how fibers running through different regions might differ from one another in terms of their anatomical origins and destinations or of their functional significance. Tractography models provide this trajectory information but these models are typically visually dense and it is difficult to ascertain anatomical subdivisions.

Therefore, in order to understand the potential anatomical and clinical utility our methods and how and if they can mitigate some of the problems discussed above, we asked two neuroscientists to evaluate our methods. We report a summary of their response. Their feedback shows that three visualization methods presented in this paper provide complimentary information about the structure of CC that maximizes their advantage of scalar and tractographic representations while minimizing their limitations. As such, the potentially provide a major advance over current visualization methods. Our methods allow to quickly ascertain anatomical subdivisions of the corpus callosum (*Bohemian coloring*), to define distinct boundaries between them (*edge rendering*), and then to view at a finer level of detail (*icon layering*), variations in fiber trajectory within larger anatomical regions. They allow researchers to do this with visual ease without the visual clutter of a tractography model. The methods will help researchers empirically define anatomical subregions whereas current methods for dividing the CC are somewhat arbitrary.

According to our experts, the methods have a number of potential applications. They could be quite valuable in training neuroscientists in white matter anatomy and individual variability. They might have particular relevance to the study of brain development and could help answer a number of intriguing anatomical and clinical questions. For example, how what are the effects of maturation (or aging) on the size and shape of CC subdivisions or in the variability of their fiber trajectories? What are the functional correlates of the fibers? Do certain disorders (e.g., dyslexia, autism) have derangements in the trajectories, number, or size of callosal fibers? What are the anatomical correlates of interhemispheric transfer of information in disorders such as generalized seizure disorder, alcoholism, schizophrenia, etc.? How what is the impact of waxing and waning white matter inflammation such as occurs in multiple sclerosis of HIV on callosal fiber structure and integrity?

The experts pointed at limitations due to tracking algorithms as well. For example, errant fibers in the tractography models will presumably get mapped onto these visualization schemes. If so, how can they be identified and culled when trying to identify distinct tracts. Also, it is clear that the boundaries between subdivisions

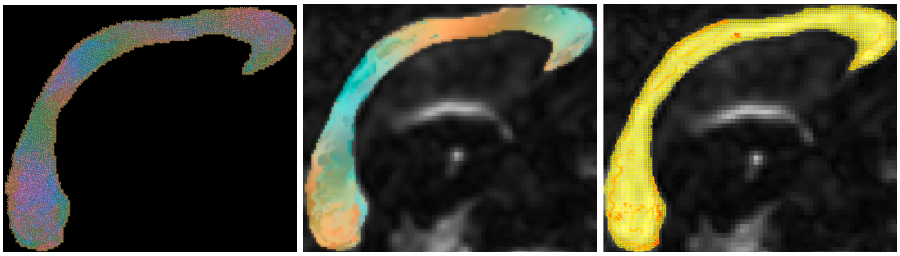

Figure 8: *Icon layering* (left), *Bohemian coloring* (middle) and *edge rendering* (right) visualizations of the mid-saggital plane of the corpus callosum in a normal volunteer's brain.

suggested by the color models are not always borne out on the edge detection models raising questions about where to define such boundaries for subregion analysis.

4 Conclusions

We have presented three cross-sectional visualization methods for DTI volumes. The primary strength of these methods is providing a compact and contextual visualization by bringing higher dimensional connectivity information onto a 2D plane which is effective and familiar to practitioners. We have applied them to visually segment the mid-saggital cross-section of the corpus callosum in the brain. Feedback from neuroscientist collaborators suggests that our visualization methods can be useful in identification of smaller caliber anatomically or functionally related white-matter structures, particularly those that are contained within large bundles or fasciculi that project to multiple areas.

We have also proposed flat-torus as a new geometric model for bivariate color mapping. Flat-torus provide a natural mechanism for continuous cyclic mappings, easing the color "bandwidth" limitations due to the shape of the color space used and the skewed distribution of the data values mapped. This, in turn, provides a mechanism to adjust sensitivity of color mapping as desired. Using the flat-torus model with two different projections to the L*a*b* color space, we introduced two continuous 2D color mapping techniques that provide approximate perceptual uniformity and can be repeated an arbitrary number of times in both directions to increase sensitivity.

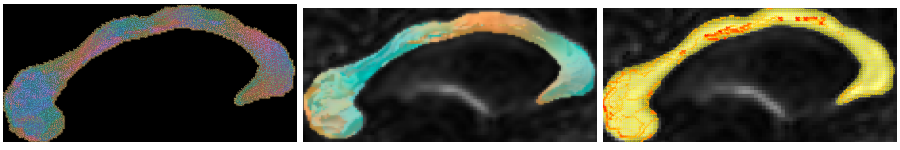

Figure 9: *Icon layering* (left), *Bohemian coloring* (middle) and *edge rendering* (right) visualizations of the mid-saggital plane of the corpus callosum in a normal volunteer's brain.

All of the three sectional visualization can be easily extended to visualization of other vector, tensor or multi-scalar data volumes. Furthermore, the underlying idea of this work, computing similarities between model primitives (geometric or otherwise) that represent how a ROI in a data set relates to the other regions and then incorporate the similarity information to the visualization of the ROI, can be applied to data and information visualization problems in different fields effectively.

5 Acknowledgements

This work was partly supported by grants from NIH (EB4155) and NSF (CNS-0427374).

References

[1] A. Cockburn and B. McKenzie. Evaluating the effectiveness of spatial memory in 2d and 3d physical and virtual environments. In *CHI'02*, pages 203–210, 2002.

[2] C. Demiralp, C. Jackson, D. Karelitz, S. Zhang, and D. H. Laidlaw. Cave and fishtank virtual-reality displays: A qualitative and quantitative comparison. *IEEE TVCG*, 12(3):323–330, 2006.

[3] C. Demiralp, S. Zhang, D. Tate, S. Correia, and D. H. Laidlaw. Connectivity-aware sectional visualization of 3DDTI volumes using perceptual flat-torus coloring and edge rendering. In *Proceedings of Eurographics*, 2006.

[4] M. P. do Carmo. *Differential Geometry of Curves and Surfaces*. Prentice-Hall, 1976.

[5] B. Moberts, A. Vilanova, and J. J. van Wijk. Evaluation of fiber clustering methods for diffusion tensor imaging. In *Procs. of Vis'05*, pages 65–72, 2005.

[6] D. M. Savage, E. N. Wiebe, and H. A. Devine. Performance of 2d versus 3d topographic representations for different task types. In *HFES Annual Meeting*, 2004.

[7] J. Sobel. Scivl: A descriptive language for 2D multivariate scientific visualization synthesis. Technical Report CS-03-24, Master's Project, Computer Science Department, Brown University, Providence, RI, 2003.

[8] S. Zhang, C. Demiralp, and D. H. Laidlaw. Visualizing diffusion tensor MR images using streamtubes and streamsurfaces. *IEEE TVCG*, 9(4):454–462, 2003.